Surface Science 605 (2011) L6–L11

Contents lists available at ScienceDirect

Surface Science

journal homepage: www.elsevier.com/ locate/susc

Surface Science Letters

Nano-structures developing at the graphene/silicon carbide interface

S. Vizzini [a], H. Enriquez [a], S. Chiang [a,b], H. Oughaddou [c], P. Soukiassian [a,*]

[a] CEA, Centre d'Etudes de Saclay, Laboratoire SIMA, DSM-IRAMIS-SPCSI, Bât. 462, 91191 Gif sur Yvette Cedex, France and Université de Paris-Sud, 91405 Orsay Cedex, France
[b] Department of Physics, University of California-Davis, CA 95616-8677, USA
[c] Université de Cergy-Pontoise, 95031 Cergy-Pontoise Cedex, France

ARTICLE INFO

Article history:
Received 12 October 2010
Accepted 5 January 2011
Available online 11 January 2011

Keywords:
Scanning tunneling microscopy
Scanning tunneling spectroscopy
Semiconductor–semiconductor interfaces
Surface defects
Silicon carbide
Graphene

ABSTRACT

We use scanning tunneling microscopy and spectroscopy to study defects on epitaxial graphene grown on a 4H-SiC(000-1) C-face substrate. At the graphene/SiC interface, we discover a few isolated small areas covered by nano-objects confined vertically and forming mesas, suggestive of packed carbon nanotubes and leading to electronic interface states. Nano-crack defects are also found at the SiC surface. They are covered with an unbroken graphene layer going deep into the crack showing no electronic interface state, and thus would probably not affect the carrier mobility.

Graphene is a single atomic layer of graphite, which can be epitaxially grown on substrates or exfoliated, and is now very well known to have outstanding properties [1–10]. Because silicon carbide (SiC), a IV–IV compound semiconductor, has a wide band gap (ranging from 2.4 to 3.3 eV depending on polytype) [11,12], epitaxial graphene grown on a SiC substrate is promising for future electronics applications [3–10,13–15] and has indeed been added to the Roadmap of Semiconductor Technology. Such epitaxial growth on hexagonal 6H/4H-SiC(0001)/(000-1) Si- and C-faces, and cubic 3C-SiC(100) has been shown to achieve graphene layers or nanoribbons [3–10,13–15]. Their atomic/electronic structures and transport properties have been determined using advanced experimental techniques, and state-of-the-art theoretical calculations [3–10,13–23]. On the C-face, graphene multilayers can be grown with each layer decoupled from one other [9,21,22], leading to unprecedented high carrier mobility of up to 250,000 cm^2/Vs at room temperature [16,18] and 200,000 cm^2/Vs elevated temperatures [17,18]. In contrast, a single graphene layer epitaxially grown on a C face SiC substrate has significantly lower mobility of 20,000 cm^2/Vs [23], possibly due to the poor quality of the graphene/SiC interface as a result of harsh graphene growth conditions. Strain is the driving force in SiC surface ordering, leading to complex surface reconstructions for both Si and C faces [11,12,24–26] leading to self-organized Si [11,27] and C [11,28] nanostructures but also to result in nano-crack defects [29]. Indeed, so far little is known about graphene/SiC interfaces where defects could affect the carrier transport properties.

In this letter, we use scanning tunneling microscopy and spectroscopy (STM/STS) to investigate at the atomic scale two types of defects at graphene/SiC interfaces and their possible effects on the electronic properties. We find nano-objects laterally confined by and below the graphene layer on top of the SiC surface, with height profiles suggestive of carbon nanotubes (CNT). We also find nano-crack defects on the SiC surface that are covered by the graphene layer. The nano-object defect leads to specific electronic interface states that may be detrimental to the graphene transport properties. In contrast, the nano-crack defects show no such interface states, with no modification of the STS spectral response, and should not affect the transport properties.

The STM/STS experiments are performed using a variable-temperature Omicron instrument at pressures in the low 10^{-10} Torr pressure range. Graphene was grown on top of a C-face 4H-SiC(000-1) n-doped at $10^{-16}/cm^3$ substrate (Cree) by thermal Si sublimation, similar to well-established procedures [19,20]. Additional Raman spectroscopy experiments were performed at the GES, CNRS-Université de Monpellier-II on the same samples. Single and double graphene layers are identified from the characteristic bright honeycomb and bright centered hexagonal atomic array seen in STM topographic images on both the Si-terminated [19,30] and C-terminated [20,21] faces of SiC. The sample was annealed to 1300 °C in ultrahigh vacuum (UHV) for 2 min, leading to the formation of the structures observed here.

We first look at the graphene surface, which has a few isolated areas exhibiting nano-objects. Fig. 1 displays representative STM topographs of a single graphene layer grown on a stepped SiC surface showing an area (420×200 nm^2) in the center having a network of

* Corresponding author. CEA, Centre d'Etudes de Saclay, Laboratoire SIMA, DSM-IRAMIS-SPCSI, Bât. 462, 91191 Gif sur Yvette Cedex, France and Université de Paris-Sud, 91405 Orsay Cedex, France.
E-mail address: patrick.soukiassian@cea.fr (P. Soukiassian).

0039-6028/$ – see front matter © 2011 Elsevier B.V. All rights reserved.
doi:10.1016/j.susc.2011.01.006

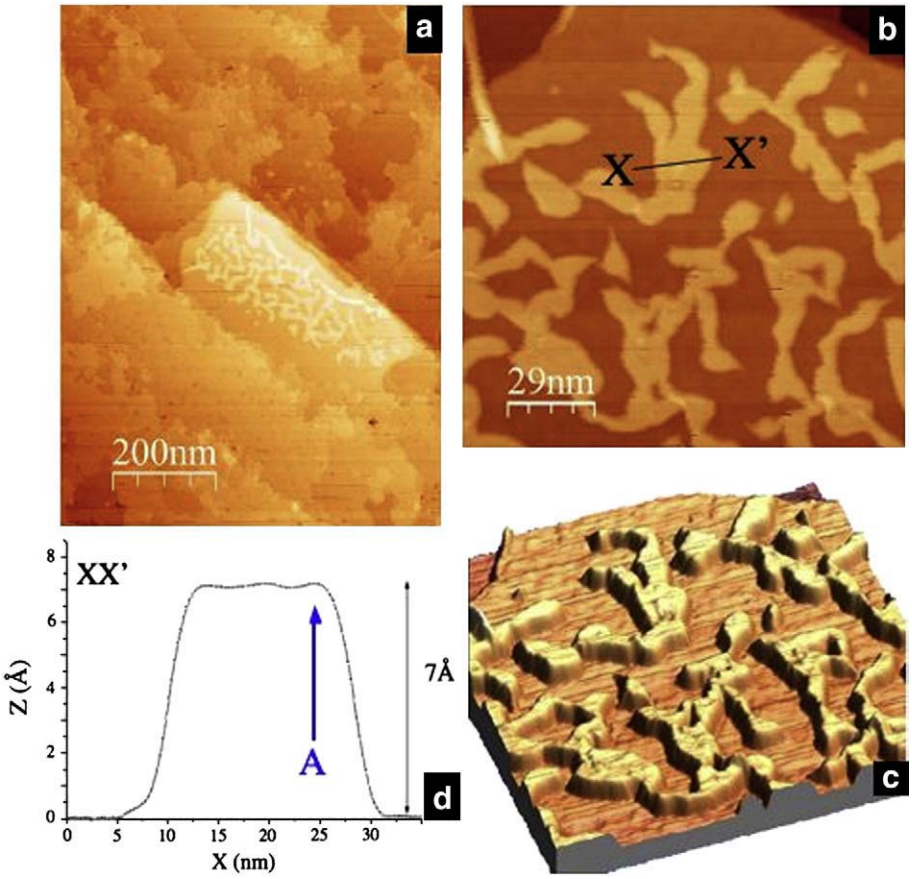

Fig. 1. a) STM topograph (750×1030 nm^2) showing an area having nano-objects at the graphene/SiC interface (U = 0.5 V, I = 0.15 nA); the A arrow shows an edge of the mesa. b) STM topograph (143×143 nm^2) of nano-objects forming mesas below the graphene layer (U = 0.6 V, I = 0.2 nA); c) 3D view of the same as in b); d) Height profile along XX' showing the mesa nature of these nano-objects (at 7 Å high) with sharp vertical sides.

these bright nano-objects. The higher resolution image (Fig. 1b) indicates more clearly the extraordinary shapes of these nano-objects, with the 3D view (Fig. 1c) showing that these nano-objects form mesas all having the same height on top of the SiC surface. A representative height profile along XX' (Fig. 1d) reveals these nano-objects to have a nearly constant height of about 7 Å, extremely steep sides, and very flat tops.

In order to determine whether these nano-objects are covered by graphene, we now change the tunneling conditions. In Fig. 2a and a', we observe the characteristic honeycomb structure of a single graphene layer, which covers not only the nanostructures but also the whole surface as a continuous single atomic layer. Fig. 2b and b' provide a similar view of a representative area without such nano-objects. This area consists of a graphene sheet covering the SiC surface and exhibits the well-established honeycomb structure of a single graphene layer with the Moiré characteristic of the coupling with the substrate (Fig. 2b') [19–21,30].

Upon heating SiC, Si sublimates, leaving excess carbon species that bond as sp^2 to form graphene. Due to the harsh growth conditions using elevated temperatures, and UHV, some possible species that could be trapped below the graphene layer are Si, C that did not form graphene, or SiC. Si species trapped below the graphene layer would most likely form two-dimensional (2D) atomic layers, and even 3D Si objects are very unlikely to exhibit the observed shape with its sharp vertical sides. SiC bi-layers have been identified below epitaxial graphene at step edges [34], while the present nano-objects form on the terraces only. The height (7.5–8 Å) of the bilayers appears close to that of the present nano-objects, but the "curly" shape (Fig. 1) of the latter looks very different and is not consistent with SiC formation [31]. Instead, the striking square cross-sectional shape of these nano-objects (Fig. 1b) suggests that the most plausible explanation is that they are formed of carbon nanotubes (CNT), which grow vertically during graphene formation and remain trapped below the graphene sheet. Indeed, CNT are known to grow perpendicularly to the SiC substrate C-face [32], and the annealing temperature used here corresponds to the temperature threshold found for CNT formation in the earlier studies, supporting such an interpretation. In addition, nanocaps have been observed from the decomposition of the C-face of SiC at 1250 °C and are considered as precursors for the formation of CNTs [32]. These have been observed as small grains with diameter of 2–4 nm and convex structure in STM measurements of this surface [32]. Not surprisingly, these structures are very different from the rough surfaces found after heating the Si face of SiC in UHV, which results in the formation of pits and steps [33].

To gain additional insights, we now perform STS measurements, with Fig. 2c giving the measured I(V) curves, showing the Schottky barrier character of the graphene layer for both monolayer graphene on SiC (black squares) and on top of a nano-object (red circles). These results, however, indicate a significant difference in the slope for positive bias, suggesting that the nano-objects are likely to induce new unoccupied electronic states at the graphene/SiC interface.

Fig. 2c' displays the (dI/dV)/(I/V) derivative curve, providing the local density of states for both graphene-covered SiC and graphene-covered nano-objects for the same representative areas of the sample as in Fig. 2c. The graphene-covered nano-objects exhibit three new spectral features, two in the valence band (IS 1, IS 2) and one in the conduction band (IS 3). IS 3 is located at 100 meV above E_F, while IS 2 and IS 1 are located at 85 meV and 150 meV respectively below E_F. Note that the only significant spectral feature for the graphene-covered SiC is peak M, located at 120 meV above E_F. IS 3 has a very

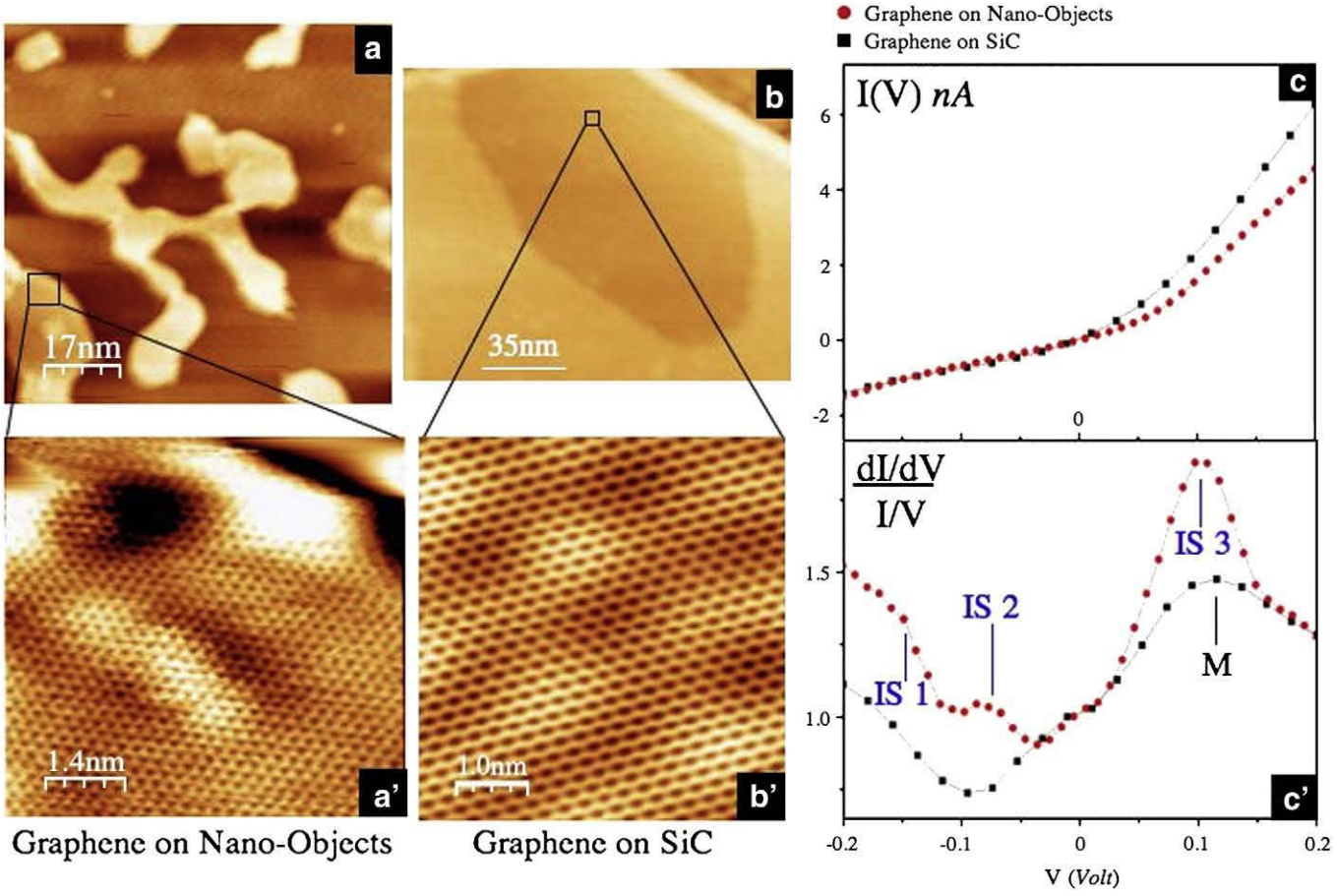

Fig. 2. a) STM topograph (87×87 nm^2) of nano-objects (U = −0.1 V, I = 0.2 nA); a') Detailed 7.2×7.2 nm^2 topograph showing the characteristic pattern of a single graphene layer covering a nano-object (U = −0.1 V, I = 0.2 nA); b) STM topograph (160×160 nm^2) of a single graphene layer covering a SiC surface (U = −0.6 V, I = 0.2 nA); b') Detailed 5×5 nm^2 area of b) showing the characteristic pattern of a single graphene layer covering SiC (U = −0.2 V, I = 0.1 nA); c) STS I(V) characteristics of single graphene layer on SiC (black squares) and graphene covering a nano-object (red dots); c') STS (d(I)/d(V))/(I/V) characteristics for the same area as in c).

different line shape from peak M, including a much larger intensity and a full-width-at-half-maximum (FWHM) of ≈80 meV, about 30% smaller than peak M. Therefore, IS 3 is unlikely to be derived from peak M and has a different character due to the underlying nanostructure. It is an empty electronic interface state, which may affect electron carrier mobility, while the filled interface states, IS 2 and IS 1, would rather influence the hole carrier mobility. Recent calculations have predicted that strain influences graphene nanoribbon conductance [34] which would be consistent with the occurrence of these electronic interface states.

The IS 3 feature in the conduction band could possibly result from "open" CNT below the graphene layer, since C atoms located at the top of an open CNT would have empty dangling bonds influencing the graphene layer just above subsequently leading to electron depletion. Such a situation will not take place for a capped CNT (which would have its end-bonds all satisfied), suggesting that IS 3 results primarily from the interaction between uncapped CNT nano-objects and the graphene layer. In contrast, IS 1 and IS 2 in the valence band could possibly result from "capped" CNT, with filled electronic orbital overlap occurring at the graphene/capped CNT interface as the most plausible explanation. Since CNT grown vertically on a 4H-SiC(000-1) surface are generally capped [32], the present results suggest that, while a similar growth is taking place below a graphene layer, some of the CNT seem to have an open termination.

Now, it is interesting to compare the occurrence of these electronic interface states in the area where graphene is covering nano-objects to recent Full Linear Augmented Plane Wave (FLAPW) *ab-initio* calculations performed on epitaxial graphene grown on the Si-face of SiC(0001) [35]. Together with atom-resolved STM measurements performed with a W-Fe tip, this work shows that the single layer graphene epitaxially grown on the SiC(0001) Si-face is a warped layer having defects. The FLAPW calculations also predict these defects to result in two electronic states below E_F at K point [35]. Despite the fact that, in our work the graphene layer is grown on a C-face SiC (000-1) substrate with a graphene/SiC interface most likely different from the corresponding Si-face, the similarity between the two electronic states predicted by the theory with the two states IS 1 and IS 2 identified by STS below the Fermi level (Fig. 2c') is striking. Indeed, it suggests that these states may have their origin from the graphene layer also warped at the edges of the nano-object "mesas" — see Fig. 1d, arrow A. Therefore, this could be at the origin of the IS 1 and IS 2 electronic interface states observed here by STS.

One should also mention that if these nano-objects were made of SiC bi-layers such as those suggested in Ref. [35], the spectroscopic STS response would be exactly the same as for a regular surface of SiC covered by graphene, with no interface states. Thus, the observed interface states further rule out the possibility that these nano-objects consist of three SiC bi-layers.

Raman spectroscopy experiments were performed to explore further the character of these nano-objects. While the results show two bands centered at ≈1380 and 1600 cm^{-1}, in good agreement with CNTs grown on the SiC substrate [36], these bands also agree

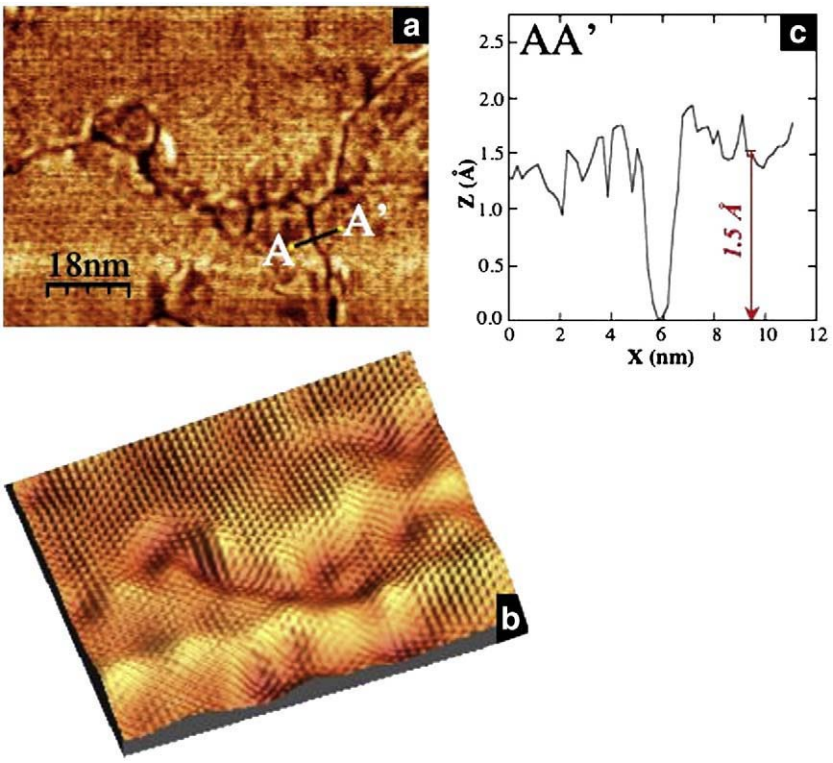

Fig. 3. a) STM topograph (91×58 nm^2) of a single graphene layer covering an area having cracks ($U = -0.1$ V, $I = 0.1$ nA); b) 3D topograph (Fourier filtered transform) for the same area as in a); c) Height profile above a crack along XX'.

with Raman measurements indicating damaged graphene [37]. Thus, Raman spectroscopy cannot distinguish between CNTs or damaged graphene, and the observed spectroscopic features are probably due to both. Such a situation is perfectly consistent with our STM and STS results, particularly with the presence of interface states clearly indicating damaged/warped graphene above these nano-objects.

We now look at nano-crack defects at the graphene/SiC interface. Such defects are known to develop on SiC surfaces [29]. Fig. 3a displays a 2D topograph of a representative area exhibiting cracks, with the height profile along AA' (Fig. 3c) showing that the crack depth is 1.5 Å and its width is 1.1 nm. Fig. 3b shows a 3D Fourier transform-filtered image of the same area, displaying everywhere the characteristic honeycomb pattern of a single graphene layer, which is a clear evidence that the continuously uniform graphene layer goes down into the crack. This behavior is consistent with the very high mechanical strength of graphene as the most resistant material ever measured [38]. Furthermore, molecular dynamics simulations on graphite fracture have shown that cracks develop along the main crystallographic directions, i.e. along the zig-zag or armchair directions [39], similar to the case of cubic and hexagonal SiC [29]. An epitaxial graphene layer on SiC has its crystallographic directions rotated from those of the 4H-SiC(000-1) substrate [21]; together with the very high mechanical resistance of graphene, this probably explains why a crack developing on the SiC surface does not extend to the graphene layer.

Fig. 4a and b displays 2D and 3D STM topographs of another representative area exhibiting cracks but covered by a double graphene layer, as shown by the characteristic centered hexagonal atomic pattern of bright spots, corresponding to every other atom in the top graphene layer, in the 6×6 nm^2 inset of Fig. 4a. The 3D image (Fig. 4b) shows that ripples occur at the crack edges. One can see a very long 1D crack (over 250 nm) along the diagonal of the images and an island of about 65×50 nm^2 surrounded by cracks near the top of the topograph (Fig. 4a and b). The representative height profile along XX' (Fig. 4c) shows that the crack depth is 3 Å, with ridges of about 1 Å high on one side and 4 Å high on the other side. These ridges likely result from graphene ripple formation at the crack edges, which could be caused by the very different expansion coefficients of graphene and SiC. In contrast to SiC, the graphene temperature dilation coefficient is negative [40], leading to a compressive strain in the graphene layer [41]. Thus, these ripples probably develop when the substrate cools down after graphene formation at high temperature.

We next use STS to explore whether such crack defects at the SiC substrate would also result in electronic interface states like those of the nano-objects described above, despite the fact that graphene sheet is not broken. Fig. 4d displays (dI/dV)/(I/V) measurements for graphene covering a crack (top), and a crack-free surface (bottom). The two (dI/dV)/(I/V) curves are very similar with no specific electronic state showing above the cracks. Thus, unlike the above CNT nanostructures, these crack defects located below the graphene layer are unlikely to have detrimental effects on the carrier mobility. Compare this case with the continuous graphene layer over the CNT nano-objects, which clearly exhibits electronic interfaces states.

In conclusion, we have evidenced two types of nanostructure defects at the graphene/SiC interface. The first are nano-objects, most likely made of CNTs, laterally confined by the graphene layer, forming mesas with a constant height, and exhibiting electronic interface states, which could have detrimental effect on the transport properties. Nevertheless, because the few such covered areas at the graphene/SiC interface are significantly distant from each other, they should not seriously affect the carrier mobility, as the graphene would have other conduction channels. Nano-cracks are another type of defect at the SiC surface. The graphene layer conforms to the cracks without breaking or resulting in electronic interface states; therefore, these are unlikely to affect the transport properties. Thus, graphene is not only the strongest known material, but also a highly pliable one, able to adapt to tall nano-objects as well as to deep nano-cracks without disruption. Graphene therefore appears as a unique

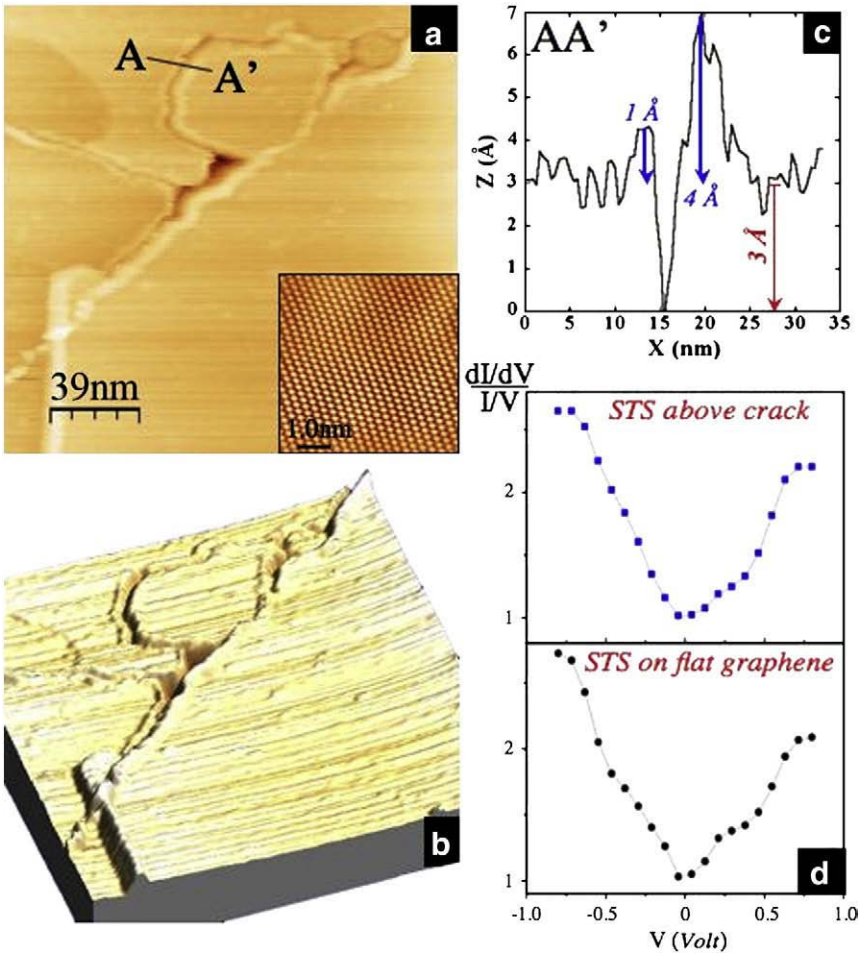

Fig. 4. a) STM topograph (194 × 194 nm^2) of a double graphene layer area covering cracks located at the SiC surface (U = 0.9 V, I = 0.2 nA) with the inset showing an area (6 × 6 nm^2) with the characteristic Moiré pattern; b) 3D picture of the same area as in a); c) Height profile above a crack along XX' showing a 3 Å depth; d) Bottom: STS (d(I)/d(V))/(I/V) characteristics on a double layer graphene on a flat SiC surface and d) Top: STS (d(I)/d(V))/(I/V) characteristics on a double layer graphene above cracks.

semiconductor, which is only slightly affected by these types of defects, despite the harsh growth conditions. We gain insight into one of the central issues of semiconductor science and technology, namely the ability to understand the interface.

Acknowledgements

This work is supported by the Agence Nationale pour la Recherche (ANR) through the GraphSiC project. We are grateful to J.-R. Huntzinger and J. Camassel from GES, UMR CNRS-Université de Montpellier II for Raman spectroscopy measurements and useful discussions.

References

[1] I. Forbeaux, J.-M. Themlin, J.-M. Debever, Phys. Rev. B 58 (1998) 16396; A.J. Van Bommel, J.E. Crombeen, A. Van Tooren, Surf. Sci. 48 (1975) 463.
[2] K.S. Novoselov, et al., Science 306 (2004) 666.
[3] C. Berger, et al., J. Phys. Chem. B 108 (2004) 19912; Science 312 (2006) 1191.
[4] K.V. Emtsev, et al., Nat. Mater. 8 (2009) 203.
[5] M. Sprinkle, P. Soukiassian, W.A. de Heer, C. Berger, E.H. Conrad, Phys. Status Solidi RRL 3 (2009) A91.
[6] N. Camara, et al., Phys. Rev. B 80 (2009) 125410; J. Phys. D Appl. Phys. 43 (2010) 374011.
[7] J. Boeckl, W.C. Mitchel, E. Clarke, R.L. Barbosa, Weijie Lu, Mater. Sci. Forum 645 (2010) 573.
[8] H. Hibino, H. Kageshima, M. Nagase, J. Phys. D Appl. Phys. 43 (2010) 374005; S. Tanaka, K. Morita, H. Hibino, Phys. Rev. B 81 (2010) 041406(R).
[9] M. Sprinkle, et al., J. Phys. D Appl. Phys. 43 (2010) 374006.
[10] J.-Y. Veuillen, et al., J. Phys. D Appl. Phys. 43 (2010) 374008.
[11] P. Soukiassian, H. Enriquez, J. Phys. Condens. Matter 16 (2004) S1611, and ref. therein.
[12] K. Heinz, J. Bernhardt, J. Schardt, U. Starke, J. Phys. Condens. Matter 16 (2004) S1705, and ref. therein.
[13] C. Virojanadara et al., Phys. Rev. B 78 (2008) 245403; C. Riedl, C. Coletti, U. Starke, Phys. D: Appl. Phys. 43 (2010) 374009; C. Virojanadara, R. Yakimova, A.A. Zakharov, L.I. Johansson, *ibid* 374010.
[14] V.Yu. Aristov, et al., Nano Lett. 10 (2010) 992.
[15] M. Suemitsu, H. Fukidome, J. Phys. D Appl. Phys. 43 (2010) 374012.
[16] M. Orlita, et al., Phys. Rev. Lett. 101 (2008) 267601.
[17] D.L. Miller, et al., Science 324 (2009) 924.
[18] W.A. de Heer, et al., J. Phys. D Appl. Phys. 43 (2010) 374007.
[19] P. Mallet, et al., Phys. Rev. B 76 (2007) 041403R.
[20] F. Hiebel, P. Mallet, F. Varchon, L. Magaud, J.-Y. Veuillen, Phys. Rev. B 78 (2008) 153412.
[21] J. Hass, et al., Phys. Rev. Lett. 100 (2008) 125504.
[22] M. Sprinkle, et al., Phys. Rev. Lett. 103 (2009) 226803.
[23] Wu. Xiaosong, et al., Appl. Phys. Lett. 95 (2009) 223108.
[24] F. Semond, et al., Phys. Rev. Lett. 77 (1996) 2013; M. D'angelo, et al., Phys. Rev. B 68 (2003) 165321; A. Tejeda, et al., Phys. Rev. B 70 (2004) 045317.
[25] P. Soukiassian, et al., Phys. Rev. Lett. 78 (1997) 907; A. Tejeda, et al., Phys. Rev. B 75 (2007) 195315.
[26] V. Derycke, P. Soukiassian, A. Mayne, G. Dujardin, Surf. Sci. Lett. 446 (2000) L101.
[27] P. Soukiassian, F. Semond, A. Mayne, G. Dujardin, Phys. Rev. Lett. 79 (1997) 2498; L. Douillard, V.Yu. Aristov, F. Semond, P. Soukiassian, Surf. Sci. Lett. 401 (1998) L395; V.Yu. Aristov, L. Douillard, P. Soukiassian, Surf. Sci. Lett. 440 (1999) L 825.
[28] V. Derycke, P. Soukiassian, A. Mayne, G. Dujardin, J. Gautier, Phys. Rev. Lett. 81 (1998) 5868.
[29] F. Amy, P. Soukiassian, C. Brylinski, Appl. Phys. Lett. 85 (2004) 926; P. Soukiassian, F. Amy, C. Brylinski, T.O. Mentes, A. Locatelli, Mater. Sci. Forum 556 (2007) 481.
[30] H. Yang, et al., Phys. Rev. B 78 (2008) 041408R.
[31] L.B. Biedermann, et al., Phys. Rev. B 79 (2009) 125411.

[32] M. Kusunoki, T. Suzuki, C. Honjo, H. Usami, H. Kato, J. Phys. D Appl. Phys. 40 (2007) 6278, and Ref. therein;
T. Maruyama, et al., Chem. Phys. Lett. 423 (2006) 317;
H. Bang, et al., Jpn. J. Appl. Phys. 45 (2006) 372;
M. Kusunoki, C. Honjo, T. Suzuki, T. Hirayama, Appl. Phys. Lett. 87 (2005) 103105;
M. Kusunoki, T. Suzuki, T. Hirayama, N. Shibata, K. Kaneko, Appl. Phys. Lett. 77 (2000) 531;
M. Kusunoki, M. Rokkaku, T. Suzuki, Appl. Phys. Lett. 71 (1997) 2620.
[33] J.B. Hannon, R.M. Tromp, Phys. Rev. B 77 (2008) 241404(R).
[34] R. Rasuli, H. Rafii-Tabar, A. Iraji zad, Phys. Rev. B 81 (2010) 125409.
[35] Y. Qi, S.H. Rhim, G.F. Sun, M. Weinert, L. Li, Phys. Rev. Lett. 105 (2010) 085502.
[36] J. Boeckl, W.C. Mitchel, Weije Lu, J. Rigueur, Mater. Sci. Forum 527 (2006) 1579.
[37] M.S. Dresselhaus, A. Jorio, M. Hofmann, G. Dresselhaus, R. Saito, Nano Lett. 10 (2010) 751.
[38] Changgu Lee, Xiaoding Wei, J.W. Kysar, J. Hone, Science 321 (2008) 385.
[39] A. Omeltchenko, J. Yu, R.K. Kalia, P. Vashishta, Phys. Rev. Lett. 78 (1997) 2148.
[40] Wenzhong Bao, et al., Nat. Nanotechnol. 4 (2009) 562.
[41] N. Ferralis, R. Maboudian, C. Carraro, Phys. Rev. Lett. 101 (2008) 156801.